行政院國家科學委員會專題研究計畫 期中進度報告

次 32 奈米 CMOS 元件可靠性分析，量子結構效應，與蒙地卡羅電荷傳輸模擬(第 2 年)
期中進度報告(精簡版)

計 畫 類 別 ：個別型
計 畫 編 號 ：NSC 96-2628-E-009-165-MY3
執 行 期 間 ：97 年 08 月 01 日至 98 年 07 月 31 日
執 行 單 位 ：國立交通大學電子工程學系及電子研究所

計 畫 主 持 人 ：汪大暉

處 理 方 式 ：期中報告不提供公開查詢

中 華 民 國 98 年 06 月 09 日

附件一

行政院國家科學委員會補助專題研究計畫 □ 成 果 報 告 ■期中進度報告

次 32 奈米 CMOS 元件可靠性分析，量子結構效應，與蒙地卡羅電荷傳輸模擬(2/3)

計畫類別：■ 個別型計畫　　□ 整合型計畫
計畫編號：NSC 96－2628－E －009－165－MY3
執行期間：　　97　年 08 月　01 日至　98 年 07 月 31 日

計畫主持人：汪大暉教授
共同主持人：
計畫參與人員：

成果報告類型(依經費核定清單規定繳交)：■精簡報告　□完整報告

本成果報告包括以下應繳交之附件：
□赴國外出差或研習心得報告一份
□赴大陸地區出差或研習心得報告一份
□出席國際學術會議心得報告及發表之論文各一份
□國際合作研究計畫國外研究報告書一份

處理方式：除產學合作研究計畫、提升產業技術及人才培育研究計畫、列管計畫及下列情形者外，得立即公開查詢
□涉及專利或其他智慧財產權，□一年□二年後可公開查詢

執行單位：國立交通大學電子工程學系及電子研究所

中　華　民　國　　98　年　　6　月　　9　日

次 32 奈米 CMOS 元件可靠性分析，量子結構效應，與蒙地卡羅電荷傳輸模擬(2/3)

Sub-32nm CMOS Device Reliability, Quantum Structure Effects and Carrier Transport Simulation by Using a Monte Carlo Method (2/3)

計畫編號：96-2628-E-009-165-MY3

執行期間：97 年 08 月 01 日 至 98 年 07 月 31 日

主持人：汪大暉 交通大學電子工程系教授

中文摘要

吾人利用 Luttenger-Kohn 模型計算次價電帶結構，自洽求解薛丁格及泊松方程式，應用於鍺通道之雙閘極金氧半電晶體。此外，利用蒙地卡羅(Monte Carlo)方法模擬電洞傳輸特性求得電洞遷移率。由模擬結果得知，鍺通道因為具有較低之傳導有效質量，所以具較高之電洞遷移率。此外，量子效應使得電洞遷移率在某個通道厚度下可被提升。

Abstract

The role of quantum confinement effect on hole mobility as a function of body thickness in Ge-channel DG-pMOSFETs is explored by solving the Boltzmann transport equation using the Monte Carlo method. The results show that the hole mobility of sub-20nm thickness exceeding the universal mobility can be achieved. This is attributed to an optimization of intrasubband and intersubband scattering rates.

Keywords: Luttinger-Kohn, Germanium, Double-gate, Monte Carlo simulation, hole mobility

I. Introduction

Double-gate (DG) metal oxide semiconductor field effect transistors (MOSFETs) and fin field effect transistor (FinFET) have been considered as the promising alternatives to the bulk MOSFETs in 22nm technology node and beyond [1-3] due to its immunity to short channel effect. In addition, advanced channel materials with high mobility compared to bulk Si, such as Ge [4] and III-V materials [5], also attract much attention to enhance device performance. Recently, experimental works have reported the possibility that the inversion carrier mobility can be further improved in quantum structure MOSFETs due to a subband modulation.[6-7] However, there has been little work on Ge-channel DG-pMOSFETs addressing the role of quantum confinement effect. On the other hand, as Lundstrom has pointed out [8], the channel backscattering coefficient plays an important role in determining the current drive and is strongly related to the near equilibrium mean free path, which can be extracted from a low-field mobility. As a consequence, it is crucial to explore the carrier transport properties in a scaled quantum device when an advanced channel material is used. It also can be

anticipated that the carrier scattering rate exhibits a dependence on a wavefunction distribution and a subband energy dispersion, which is varied significantly with the geometry of the quantum devices. In this work, we, therefore, analyze the quantum confinement effect on hole mobility versus body thickness (T_{Ge}) in Ge-channel DG-pMOSFETs. The low-field hole mobility is calculated by a Monte Carlo method and only phonon scattering is present. The quantum confinement effect on hole mobility in Ge-channel is compared with Si-channel.

II. Physical Model and Simulation Technique

Instead of one-mass approximation, the valence subband structures for the two-dimensional (2D) hole gas in Ge-channel DG-pMOSFETs are obtained self-consistently from the coupled Poisson and Schrödinger equations with a six-band Luttinger-Kohn Hamiltonian including spin-orbit-coupling [9]. On the other hand, the Bir-Pikus deformation potentials [10] are included to take into account the stress effect. The wavefunctions are set to zero in the Ge and gate dielectric interface, assuming that the wavefunctions do not penetrate the gate dielectric. In addition, an appropriate rotation matrix must be performed when dealing with the surface orientation other than the (100). The material parameters for both Si and Ge, including Luttinger parameters, deformation potentials, used in the calculation are given in Table I [11]-[13], respectively. Based on the calculated valence subband structures, a Monte Carlo method is then carried out to solve the Boltzmann transport equation to compute the low-field mobility. Two relevant scattering mechanisms, acoustic phonon scattering and optical phonon scattering, are considered in the simulation.

Table I. The relevant material parameters and scattering parameters used in the Monte Carlo simulation for Si and Ge, respectively. The γ_1, γ_2 and γ_3 are Luttinger parameters and Δ is the split-off energy. The a_v, b, and d are the Bir-Pikus deformation potentials. The C_{11} and C_{12} are elastic constants. The Ξ and D_tK are the average acoustic and optical deformation potential, respectively. The $\hbar\omega$ is the phonon energy.

	Material paramters								
	γ_1	γ_2	γ_3	Δ (eV)	a_v (eV)	b (eV)	d (eV)	C_{11} (dyn/cm^2)	C_{12} (dyn/cm^2)
Si	4.285	0.339	1.446	0.044					
Ge	13.38	4.24	5.69	0.297	2.0	-2.2	-4.4	1.2853x10^{12}	4.826x10^{11}

	Scattering paramters		
	Ξ (eV)	D_tK (10^{8}eV/cm)	$\hbar\omega$ (meV)
Si	9.2	13	62
Ge	11	6	38

The relaxation time approximation is used, such that scattering process can be assumed to be either vector randomizing or isotropic elastic. The formulation of the scattering mechanisms can be found in [14-15] and are described briefly as follows. The acoustic phonon scattering rate is give by

$$S_{ac} = \frac{2\pi k_B T \Xi^2}{\hbar \rho u_l^2} \cdot D_n(E) \cdot H_{mn}(k_{\|}, k_{\|}^{'})$$

where Ξ is the effective acoustic deformation potential, ρ is the material density, u_l is the sound velocity, T is lattice temperature and $D_n(E)$ is the two dimensional density of hole states in n-th subband.

The optical phonon scattering rate is

$$S_{op} = \frac{\pi (D_t K)_{op}^2}{\rho \omega_{op}^2} \cdot [n_{op} + \frac{1}{2} \mp \frac{1}{2}] \cdot D_n(E \pm \hbar\omega_{op}) \cdot H_{mn}(k_{\|}, k_{\|}^{'}) \times \frac{1 - f_0(E \mp \hbar\omega_{op})}{1 - f_0}$$

where f_0 is the Fermi-dirac distribution. D_tK is the average optical deformation potential n_{op} is

the Bose-Einstein distribution. The + and – represents the absorption and emission rates.

In the Monte Carlo simulation, a look-up table of the *E-k* relationship for the valence subbands is established. Only eigenvalues for $k_{||} < 0.6\pi/a_{Ge}$, which significantly contribute to a low-field mobility, are evaluated. A single particle Monte Carlo simulation is performed under an external electric field. The simulation procedure is continued until the fluctuation in mobility due to the statistical error is less than 0.5%.

III. Simulation Result

First of all, it should be pointed out that we use the calibrated scattering parameters of Si from a conventional Si-MOSFET and Ge from a SiGe-on-insulator device [16]. Fig. 1 shows the simulated device structure and corresponding inversion hole distribution.

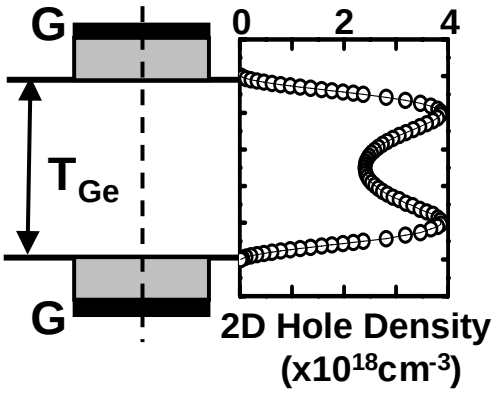

Fig. 1 Inversion hole distribution in a Ge-channel DG-pMOSFET.

Fig. 2 shows the simulated hole mobility versus body thickness in (100)/<010> Si-channel DG-pMOSFETs, where () and <> are the notations of surface orientation and channel direction, respectively. It is obvious that the hole mobility decreases monotonically with body thickness. The simulation shows similar trend with the recent experimental data [6]. However, unlike in (100) Si-channel DG-pMOSFETs, the hole mobility as a function of body thickness in Ge-channel shows an enhancement characteristic.

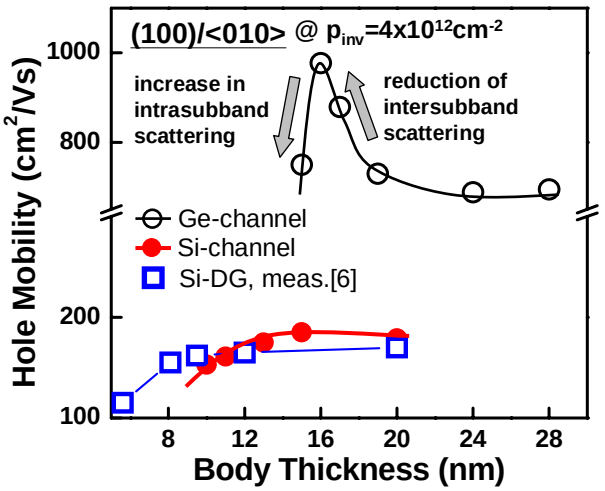

Fig. 1 Hole mobility as a function of body thickness for (100)/<010> Si- and Ge-channel DG-pMOSFETs. Only acoustic phonon and optical phonon scatterings are considered. The hole mobility enhancement is observed at a small body thickness. Note that the peak of hole mobility for Ge-channel is estimated to be about four times as large as for Si-channel.

When a body thickness is scaled down, the hole mobility increases gradually to a maximum around T_{Ge}=16nm, and then decreases drastically. Note that the calculated hole mobility at T_{Ge}=28nm is about 700 cm^2/Vs, which significantly deviates from the bulk value of Ge. Thus, we examine the hole mobility in a very low p_{inv} where it is expected to recovery the bulk mobility. However, the calculated mobility is only 67% of the bulk mobility. This is due to larger phonon deformation potentials in a MOSFET than in a bulk material, which results from stress at gate dielectric and semiconductor interface [17].

The explanation of the mobility enhancement is described as follows. As a body thickness decreases, the energy difference between the first subband and second subband increases owing to quantum confinement effect, as shown in Fig. 3, where ΔE is the energy difference between the first subband and second subband.

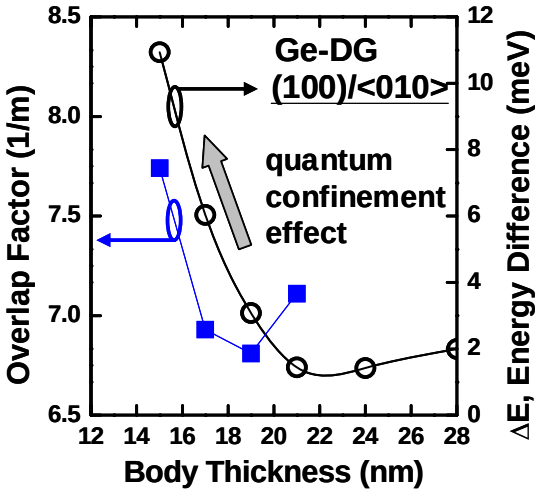

Fig. 3 The calculated overlap factor of the first subband and energy difference between the first subband and second subband in (100)/<010> Ge-channel DG-pMOSFETs. An increase in both overlap factor and energy difference at a small body thickness is due to quantum confinement effect.

Therefore, larger energy difference leads to a reduction of intersubband scattering rate, and thus favors mobility improvement. However, when a smaller body thickness is considered, there is a wider distribution in momentum space due to the uncertainty principle. This can be understood from the illustration of Fig. 4.

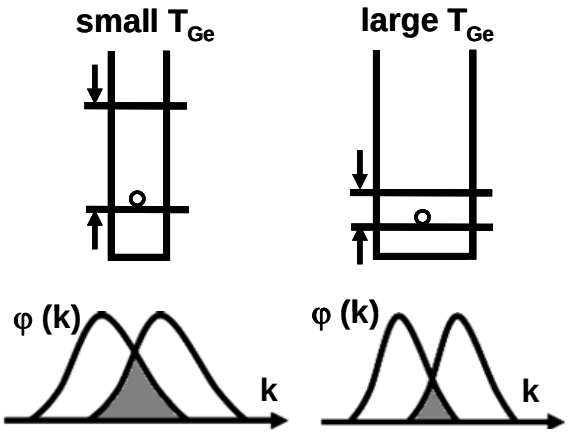

Fig. 4 Illustration of the overlap factor of an intrasubband scattering. The intrasubband scattering rate increases due to a larger overlap factor when a body thickness is reduced.

Only the shaded region contributes to the overlap factor. Thus, the spread of the wavefunction in momentum space results in a larger overlap factor and thus a larger intrasubband scattering rate. In this regime, the mobility accordingly decreases. As a consequence, there exists a window of a body thickness where the scattering rates can be minimized, giving rise to an onset of peak mobility.

IV. Summary

In summary, a two-dimensional Monte Carlo simulation is developed to explore the hole transport properties in a DG p-MOSFET. Our study indicates that the 2D hole mobility varies significantly with the geometry of the DG device. The hole mobility enhancement is about 40% for (100)/<010> due to an optimization of the intrasubband and intersubband scattering rates.

References

[1]Francis balestra, Sorin cristoloveanu, Mohcine benachir, Jean brini, and Tarek elewa, IEEE Electron Device Lett. 8, 410 (1987).

[2]H. Kawasaki, M. Khater, M. Guillorn, N. Fuller, J. Chang, S. Kanakasabapathy, L. Chang, R. Muralidhar, K. Babich, Q. Yang, J. Ott, D. Klaus, E. Kratschmer, E. Sikorski, R. Miller, R. Viswanathan, Y. Zhang, J. Silverman, Q. Ouyang, A. Yagishita, M. Takayanagi, W. Haensch, and K. Ishimaru, Tech. Dig. – Int. Electron Devices Meet. 2008, 237 (2008).

[3]T. Mérelle, G. Curatola, A. Nackaerts, N. Collaert, M. J. H. van Dal, G. Doornbos, T.S. Doorn, P. Christie, G. Vellianitis, B. Duriez, R. Duffy, B.J. Pawlak, F.C. Voogt, R. Rooyackers, L. Witters, M. Jurczak, and R. J. P. Lander, Tech. Dig. – Int. Electron Devices Meet. 2008, 241 (2008).

[4]Ruilong Xie, Thanh Hoa Phung, Wei He, Zhiqiang Sun, Mingbin Yu, Zhiyuan Cheng, and Chunxiang Zhu, Tech. Dig. – Int. Electron Devices Meet. 2008, 393 (2008).

[5]N. Goel, D. Heh, S. Koveshnikv, I. Ok, S. Oktyabrsky, V. Tokranov, R. Kambhampati, M. Yakimov, Y. Sun, P. Pianetta, C. K. Gaspe, M. B. Santos, J. Lee, S. Datta, P. Majhi and W. Tsai, Tech. Dig. – Int. Electron Devices Meet. 2008, 363 (2008).

[6]Shigeki Kobayashi, Masumi Saitoh, and Ken Uchida, Tech. Dig. – Int. Electron Devices Meet. 2007, 707 (2007).

[7]Gen Tsutsui, Masumi Saitoh, and Toshiro Hiramoto, Tech. Dig. VLSI Symp. 2005, 76 (2005).

[8]Mark S. Lundstrom, IEEE Electron Device Lett. 22, 293 (2001).

[9]J. M. Luttinger and W. Kohn, Phys. Rev. 97, 869 (1956).

[10] G. L. Bir and G. E. Pikus, *Symmetry and Strain-Induced Effects in Semiconductors* (Wiley, New York, 1974).

[11] Tony Low, M. F. Li, Y. C. Yeo, W. J. Fan, S. T. Ng and D. L. Kwong, J. Appl. Phys. 98, 024504 (2005).

[12] J. D. Wiley, Solid State Commun. 8, 1865 (1970).

[13]M. V. Fischetti, and S. E. Laux, J. Appl. Phys. 80, 2234 (1996).

[14]M. V. Fischetti, Z. Ren, P. M. Solomon, M. Yang, and K. Rim, J. Appl. Phys. 94, 1079 (2003).

[15]Marco De Michielis, David Esseni, Y. L. Tsang, Pierpaolo Palestri, Luca Selmi, Anthony G. O'Neill, and Sanatan Chattopadhyay, IEEE Trans. Electron Devices 54, 2164 (2007).

[16]Anh-Tuan Pham, Christoph Jungemann, and Bernd Meinerzhagen, IEEE Trans. Electron Devices 54, 2174 (2007).

[17]M. Lundstrom, *Fundamentals of Carrier Ttransport*, 2nd ed. (Cambridge University Press, 2000).